NONIMAGING FRESNEL LENS CONCENTRATORS FOR PHOTOVOLTAIC APPLICATIONS

Ralf Leutz[*†], **Akio Suzuki**[**], **Atsushi Akisawa**[*] **and Takao Kashiwagi**[*]

[*]Tokyo University of Agriculture and Technology,
Department of Mechanical Systems Engineering
2-24-16 Naka–cho, Koganei–shi, Tokyo 184-8588, Japan
[†]email ralf@star.cad.mech.tuat.ac.jp, phone/fax +81-42-388-7076

[**]UNESCO,
Bouvin 3.26 SC/EST, 1, rue Miollis, 75732 Paris Cedex 15

Abstract – This study aims at clarifying the role of color aberrations in a novel nonimaging Fresnel lens of moderate concentration, intended for photovoltaic applications where homogeneous illumination is imperative. Refraction does indeed lead to color aberrations, but these are eliminated by rays of different color mixing on the absorber due to the nonimaging nature of the lens. Additionally, the manufacturing of the lens prototype, its working principle, and preliminary tests under the sun and under the moon are explained. An introduction deals with the metaphorical separation of photovoltaic concentration by means of lenses on the one hand, and solar thermal concentration with mirrors on the other.

1 PHOTOVOLTAIC OR SOLAR THERMAL CONCENTRATION?

When we had completed the design simulation of a nonimaging Fresnel lens solar concentrator, we thought of it as being a direct competitor to the Compound Parabolic Concentrator (CPC). We still think this to be true, but the title of this paper states that this paper is investigating the role of our Fresnel lens in photovoltaic applications. Two questions arise: First, why does 'refractive lens' sound like 'pv', and 'reflective mirror' like 'solar thermal'? And second, assuming the distinction to be merely historical, why are we considering and testing our nonimaging lens for use in photovoltaic conversion of sunlight?

Boes and Luque (1992) try to illuminate why lenses have been used almost exclusively in photovoltaics, and mirrors in solar thermal systems. They point out that Fresnel lenses are offering more flexibility in optical design, thus allowing for uniform flux on the absorber, which is one of the conditions for efficiency in photovoltaic cells. Furthermore, flat Fresnel lenses are said to be less prone to manufacturing errors, since the errors at front and back faces of the prism are indeed partially self–correcting, while an angular error in the mirror's slope leads to twice this error in the reflected beam. This is true for flat Fresnel lenses, where the front faces of the prisms blend into a horizontal surface, and also for shaped lenses, in particular nonimaging lenses.

On the other hand, imaging Fresnel lenses are still very prone to movements of the focal point due to nonparaxial incidence, especially when compared to nonimaging mirrors, which have been available longer than nonimaging lenses. Ideal nonimaging concentrators are offering uniform radiation on flat absorbers, the main characteristic of 'ideal' being the condition that the first aperture of the concentrator be filled out completely by uniform radiation, or radiation from a Lambertian source. Only then the second aperture (the absorber) will receive uniform flux. The sun itself may qualify as Lambertian approximation, although its brightness is not uniform, and wavelength dependent brightness changes significantly from its center to its outer areas. Since nonimaging concentrators are designed according to one or two pairs of acceptance half angles, the concentrator accepts light other than the almost paraxial rays of the sun (acceptance half angle $\theta = 0.27°$), and concentrated flux is not uniform. Secondary concentrators can be used to make the flux on the absorber more uniform, but the price to be paid usually is rejection of at least some rays.

Imaging Fresnel lenses may be designed aspherically, and with corrections in each prism for uniform flux, but both focal forshortening and longitudinal focal movements require high precision tracking. Prisms split white light into its color components. Refraction indices are wavelength dependent, and true uniform flux will remain an illusion, although we will see that our nonimaging Fresnel lens mixes colors at the absorber.

A complete discussion of these topics can be found in Grilikhes (1997), Boes and Luque (1992), and Welford and Winston (1989). Although the authors' approach comes from different directions according to the field the are most familiar with, no clear technical link between 'lens' and 'pv' or 'mirror' and 'thermal' could be established.

Historical aspects are apt to throw more light onto these metaphorical connections. The ability to concentrate has been known for both lenses and mirrors for millenia. Fresnel lenses made of glass have been used soon after their practical discovery by Jean Augustin Fresnel in 1748 as

collimators in lighthouses. The reason for their success was that they were considerably lighter than singlets and absorbed less radiation than their oil covered mirror predecessors. Even today, lighthouse lenses are manufactured from glass to withstand the high temperatures present. Parabolic mirrors, on the other hand, had been used for large scale solar thermal applications since the beginning of the 20th century: in 1913 a 35 KW_{mech} collector field consisting of 1,233 m^2 parabolic troughs was installed in Eqypt for irrigation, before World War I destroyed further efforts in solar thermal power generation (Grasse *et al.*, 1991).

The first idea for the collection of solar energy for industry and recreation comes from Leonardo da Vinci, who in 1515 proposed a parabolic mirror four miles across. In 1866, Mouchot designed and ran a solar powered steam engine (see Kaneff, 1996). Solar air and water heating for housing application was tested and documented for four houses in the United States by the end of World War II (Löf 1992); and thermodynamic properties of solar energy collection were well researched.

The photovoltaic effect was discovered already in 1839 by Edmond Becquerel (see Green, 1992). More important, however, was the coincidence that the world saw both the invention of practical Fresnel lenses due to the availability of acylic plastic *and* the development of efficient silicon solar cells for applications in space in the early 1950's. Polymethylmetacrylate (PMMA) is a lightweight, clear, and stable polymer with optical characteristics close to those of glass, and superior utilizability for the manufacturing of Fresnel lenses. The properties of PMMA were reported during World War II by Johnson (see Oshida, 1961). Since the late 1940's experimental Fresnel lenses were build mainly for optical applications for electrotechnology, such as sensors (Miller *et al.*, 1951).

From the beginning, Fresnel lenses and photovoltaics were the domain of companies and large research institutions. The link between both fields may have been electrotechnology where experiences in pv and optical sensors are overlapping. Confusingly, the nonimaging concentrator CPC had been invented in 1965 for the reflection of Čerenkov radiation onto a sensor, and it took more than a decade for it to become the metaphor for solar thermal energy collection. The CPC found other applications in astronomy (in combination with a lens, Hildebrand, 1983), and laser technology.

The advantages of nonimaging concentrators were realized by the solar thermal community. Some research work was carried out in the development of nonimaging Fresnel lenses (Collares–Pereira, 1979; Kritchman *et al.*, 1979; Lorenzo and Luque, 1981), with the two former works aiming at solar thermal applications, but earlier failures with imaging lenses (Harmon, 1977) led lenses into thermal oblivition. Modern solar thermal markets are established, and concepts have been developed that do not include Fresnel lenses. Research institutions and companies are organized in strict separation of solar thermodynamic and solar electrotechnical departments, reinforcing the status quo.

Similarly, mirrors never found their way into the photovoltaic community and market. The imaging Fresnel lens of O'Neill (1978) is the only commercially introduced concentrator technology for photovoltaics, that we know of. It has never been published in the predominantly thermal *Solar Energy Journal*. In fact, it seems that no other lens specifically designed for photovoltaics has been made public in any journal, or patent, an indication that only ordinary imaging Fresnel lenses are used for solar cells. This paradigma has only recently been broken with the EUCLIDES project developed by Sala *et al.*, including Luque, which uses parabolic trough concentrators and bifacial cells.

Having said all this, and having found only historical reasons for a distinction between photovoltaics and solar thermal developments, why do we follow the same trodden path, and design and test a novel nonimaging Fresnel lens for photovoltaics?

The answer is: The novel nonimaging Fresnel lens has been designed with a thermal application in mind. Thermal requirements differ from those in photovoltaics. Medium temperatures can be achieved by reducing conductive and convective heat losses, tracking is more problematic due to transport of the working fluid, and 'hot spots' pose less problems. Absorber design is of some difficulty as its shape is often not flat, heat pipes or fluid operations have to be installed.

Testing the performance of the collector is relatively simple in photovoltaics, although concentrator cells must be applied, but output is easily measured, whereas solar thermal application testing requires larger collector arrays. The decision to produce a prototype with acceptance half angle pairs of a cross–sectional $\theta = \pm 2^\circ$ and a perpendicular $\psi = 12^\circ$ fell based on the potential of easier recognition of optical errors when absorber and angles are chosen smaller, and the geometrical concentration ratio is selected higher.

2 NONIMAGING FRESNEL LENS DESIGN AND MANUFACTURING

The design of the nonimaging Fresnel lens shown in Fig. 1 has been described in detail in Leutz *et al.*, 1999. Based on the priciples of edge rays, and minimum deviation prisms, under the condition of a smooth outer surface, the optimum shaped Fresnel lens has been found in a numerical simulation. The design of the line–focusing lens is based on the definition of two pairs of acceptance half angles: θ in the cross–sectional plane (the plane of the fixtures in Fig. 1), and ψ in the plane perpendicular to it.

A number of potential manufacturers in Japan, Germany and the USA were contacted concerning the prototyping of

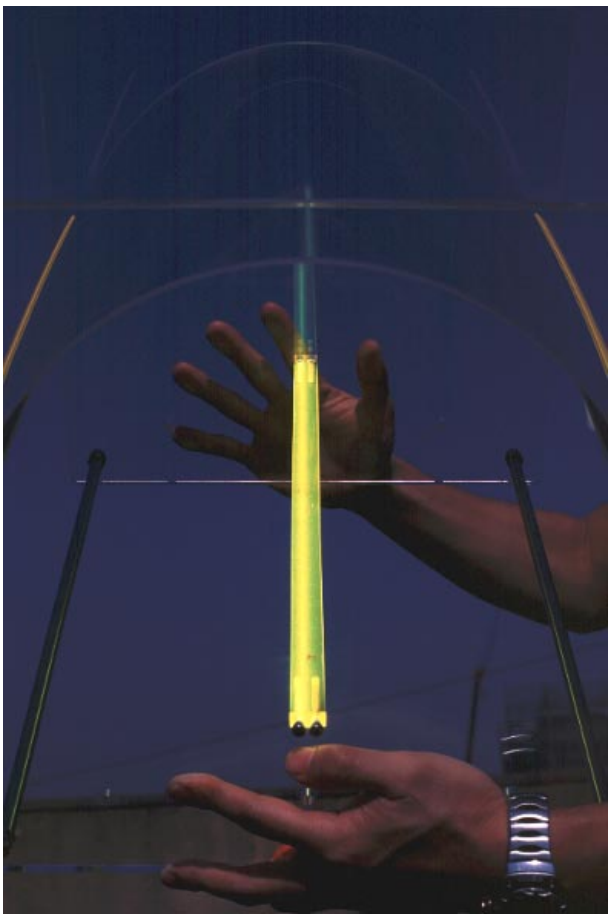

Figure 1: The first prototype of the nonimaging Fresnel lens under the sun of Tokyo, May 1999. Acceptance half angles $\theta = 2°$, $\psi = 12°$.

a Fresnel lens with given specifications. In the first round of consultations, glass as lens material (i.e. the integration of the lens and a vacuum tube) was ruled out as impractical. The second round ruled out extrusion as manufacturing method for a prototype, and found the cost for a mould for the arched lens prohibitively high. The mould for a shaped lens must feature a collapsable core due to the undercut formed by some of the prism tips.

Finally, it was decided to have the lens manufactured as flat sheet, to be bent into shape later on. A Tokyo based manufacturer was found, and the following specifications were obtained. The lens was to be of a size of 400×400 mm, moulded into PMMA of thickness 1.0 mm, with the distance in height between prism tips and grooves being smaller than 0.5 mm. All prisms of the lens should be designed in such a way that they had a common centerline, i.e. a horizontal line crossing all prisms from which the distances to each one prism's tip and groove were equal.

Contrary to common imaging designs, the prisms in this lens are not equaldistant when assembled horizontally. In the shaped version of the lens, each prism covers a angular segment similar to those formed by the spokes of a wheel, but without its circular shape. The lens to be the first prototype was chosen to be of acceptance half angles $\theta = 2°$ and $\psi = 12°$. The lens was truncated at half height based on previous findings that found the performance of a truncated lens only slightly inferior to the one of a full lens (Leutz *et al.*, 1999).

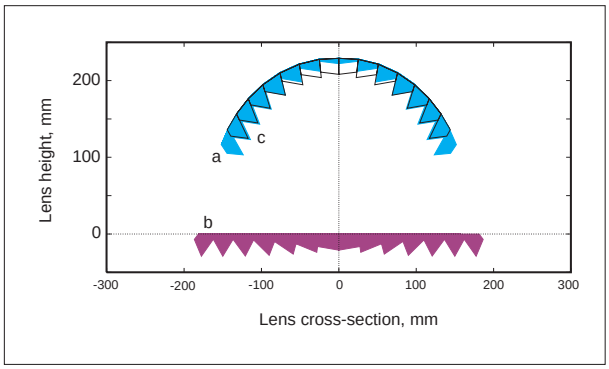

Figure 2: Preparations for manufacturing the Fresnel lens prototype. The prisms of an optimum shaped lens (a) are moved and rotated to form a flat sheet (b). Prism tips and grooves are arranged equaldistant to a centerline for ease of moulding. Resized prisms are brought back into shape (c).

The lens is prepared for manufacturing by simulating its width according to the maximum dimensions given. The absorber width is found accordingly. The number of prisms and their coordinates in the shaped lens are calculated under the restrictions of given maximum groove depth. It is helpful to be able to have an additional degree of freedom in the simulation, which is the possibility to backstep, i.e. starting a new prism from a given point on the front face of the previous one, thus avoiding the thickness of the lens to be zero at the grooves. The effects of the 1.0 mm acrylic sheet for refraction (refraction at a plane parallel plate) are dismissed as insignificant on the grounds of being very small.

In a first step (see Fig. 2a), the prisms are moved into a horizontal position, and rotated until their front faces form a smooth flat line. The second step deals with the changes necessary due to the centerline requirement. A prism is chosen to serve as reference for setting the position of the centerline. Prisms from the reference prism towards the center of the lens are increased in size in order to have their back faces (which are almost parallel to their front faces, making the prism very 'thin') cross the centerline at a point where the elevation distances between groove and tip are equal. Outward prisms are decreased in size until the same condition is fulfilled. The centerline condition facilitates ease of pressing the lens shape into a PMMA sheet. The coordinates of these prisms (Fig. 2b) are given to the manufacturer.

In a third step (Fig. 2c), the resized prisms of the flat lens are rearranged into the arched shape for two purposes. Small differences are observed in comparison to the original shape due to the resized prisms. The new lens shape must be known to first, produce a frame into which the bent lens is to be fixed and, second, to evaluate the newly shaped lens by ray tracing.

3 PRELIMINARY TESTS OF THE 02/12–LENS

The prototype of the nonimaging Fresnel lens with acceptance half angle pairs $\theta = 2^\circ$ and $\psi = 12^\circ$ has not been available long enough to permit the conduction of detailed tests. However, the lens was mounted on a test rig, and its previously simulated optical design properties could roughly be confirmed. There never had been great concern about the verification of the characteristics of the original optimum shaped lens, but we were satisfied to see that the lens manufactured as flat sheet fulfilled all expectations when bent into shape. It can be stated that the amount of material to be displaced between the prims when the lens is bent into shape does not influence the optical properties of the lens in any visible way.

Table 1: The sun and the moon as light sources for the testing of solar concentrators. Average radii, distances to earth, solid angles on 1 May 1999, 21:32 hours, in Tokyo, and relative brightness.

	Sun	Moon
Radius, m	$0.695 \cdot 10^9$	$1.73 \cdot 10^6$
Distance to earth, m	$150 \cdot 10^9$	$384 \cdot 10^6$
Solid angle (1 May 1999), °	0.5291	0.4913
Relative brigthness*	770	1

*Apparent brightness, or magnitude in visible light when celestial body in opposition, i.e. opposite side of the earth from the sun, usually closest to earth, and best visible.

In a first experiment, the lens prototype was exposed to the light of the almost full moon (99% full on 1 May 1999, when the experiment was conducted). Utilizing the sunlight reflected from the moon for measuring the optical properties of a solar concentrator offers some advantage over using the rays of the sun directly. The moon appears to have almost the same size as the sun when seen from the earth (Tab. 1). The moon's diameter is 400 times smaller than the sun's, but the moon is on average 400 times closer to earth than the sun. The image of the moon is clearly defined against a dark sky, whereas the sun appears larger, with a solid angle of 5.7° per definition filled out by beam radiation. Light entering the concentrator shows on the absorber not only bright against the dark background, but can be described as offering a clear threshold between direct rays and darkness. When concentrating sunlight during the day, the region around the sun is of almost the same brightness as the sun itself making tracing of rays in the concentrator difficult, bright light and bright absorber are sometimes difficult to distinguish.

The light reflected from the moon is 'cold' light, its intensity is too low to heat up the absorber. On the other hand, sunlight geometrically concentrated by a factor of 20, may damage a dummy absorber, or measuring device. Still, the sunlight reflected from the moon at night does have a similar spectral distribution to sunlight coming directly from the sun during the day, since the moon lacks an atmosophere that could interfere with its characterization of a grey body.

Figure 3: Testing the Fresnel lens under the 99% full moon. 1 May 1999, 21:20-21:35, Tokyo, Japan, at 35.5°N. The lens is seen from its lower right side. The see through absorber, seen from its back, and almost filled out with light, appears in the lower left corner of the picture.

A photograph of the moon over the lens is shown in Fig. 3. The see through absorber appears in the lower left corner. The photograph captures a time series of ten exposures over a period of fifteen minutes. The moon appears over the longitude of the same location on earth not every 24 hours like the sun (not taking into account analemma), but about fourty minutes later. Thus, the movement of the moon over a point on earth is slightly slower than that of the sun. Not 15° of solid angle are covered every hour, but only approximately 14.5°.

During the 15 minutes of photographic exposure in Fig. 3 the moon has covered a solid angle of some 3.5 degrees. The absorber has almost fully been covered with light concentrated by the lens, which has an acceptance half angle of $\pm 2.0^\circ$, as expected. Furthermore, the lens has been inclined towards the south, or in the perpendicular direction

to its cross–section. As will be shown later, aberrations of the refractive behaviour of the lens are smallest in this position at the perpendicular design angle $\psi = \pm 12^\circ$.

A similar test was conducted under the sun at clear skies a few days after the moon experiment (Fig. 1). With the increased brightness, the exact focal area was hard to distinguish from its immediate surroundings, but the optical properties of the lens were confirmed.

Contrary to imaging lenses under similar conditions we could not observe any color aberrations, which are common near the focal point of imaging devices. Of course, any prism refracts rays depending on wavelength, but the nonimaging lens mixes those rays in the absorber plane, and no color lines accompanying the focal area are observed.

4 REFRACTION AND WAVELENGTH DEPENDENT DISPERSION

The speed of light in a medium varies with color. Since the refractive index n of a material is defined as ratio of the speed of light in vacuum to the speed of light in a material, the refractive index is a function of the color of light, i.e. its wavelength.

$$n = n(\lambda) \tag{1}$$

Dispersion occurs due to the color–dependent refraction. Shorter wavelengths (ultraviolet, blue) are refracted further off the surface normal as longer wavelengths (red, infrared). In most cases, three wavelengths are used to describe the dispersion of an optical material. These are the spectral lines for helium at 587.6 nm (yellow light), and hydrogen at 486.1 nm (blue) as well as 656.3 nm (red light), respectively (Shannon 1997). When only one refractive index is given, usually the D–line at 589.2 nm is used (Jenkins, White 1981).

The refractive index can be plotted as a function of the wavelength for a material. This function can only be expressed empirically. The most common approach and the industrial standard since Schott abandonned its Schott dispersion formula (Shannon 1997) is called Sellmeier formula. This formula, found in 1871, is not entirely empirical but has a physical basis in describing the dispersion of uncoupled molecules (they are assumed to response with resonance to the passing light waves, and in turn alter the velocity of the light).

$$n = \sqrt{1 + \sum_{j=1}^{3} \frac{a_j \lambda^2}{\lambda^2 - b_j}} \tag{2}$$

where the wavelength λ is in μm. The refractive index of polymethylmetacrylate is sightly smaller than the one

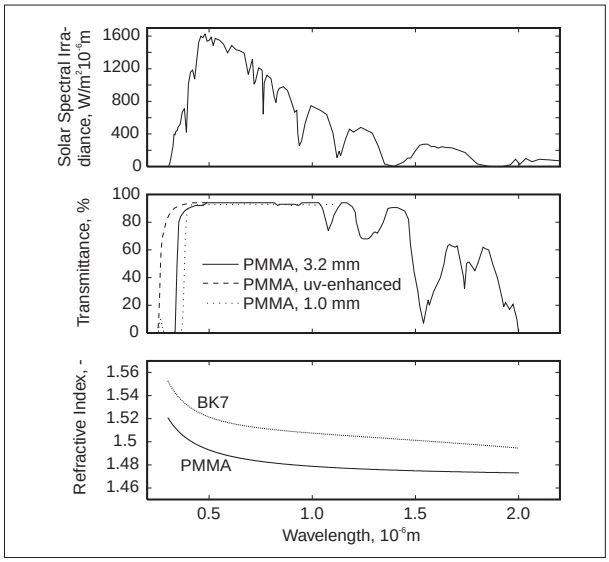

Figure 4: **Top**: Solar terrestrial spectral irradiance (IEC, USA, AM=1.5; Amakawa and Kuwano (1994)). **Middle**: Transmittance of general purpose acrylic and acrylic with enhanced transmittance for ultraviolet rays (straight and broken lines, Fresnel Technologies, 1995), dotted line authors's measurements of 1.0 mm sample. **Bottom**: Refractive indices of BK7 glass (Schott, 1992) calculated with the Sellmeier formula, and polymethylmetacrylate PMMA (Oshida, 1961) calculated with the Hartmann formula. All data plotted as function of wavelength.

presented for BK7 glass (see Fig. 4). The wavelength dependent refractive index may also be calculated with the empirical Hartmann formula. Its accuracy is limited in comparison to the Sellmeier formula, but this should not be of great concern for solar energy applications, since in the visible spectrum accuracy is sufficient. The Hartmann formula is explained for PMMA by Oshida (1961) with the constants for acrylic. λ in Å.

$$n = n_0 + \frac{C}{\lambda - \lambda_0} = 1.4681 + \frac{93.42}{\lambda - 1,235} \tag{3}$$

Data for PMMA obtained with Hartmann's formula has been plotted in Fig. 4.

Transmittance of PMMA almost reaches that of BK7 glass over the whole solar spectrum. Data for a sample of $d = 3.2$ mm analysed by Fresnel Technologies (1995) is reproduced in Fig. 4. A sample of $d = 1.0$ mm has been measured for comparison. Further measurements of a ten times thicker sample of general purpose polymethylmetacrylate show that reflection at the surface, and not absorption within the material is the leading cause for transmission losses. Reflection accounts for less than 10% of transmission losses if the angle of incidence is kept below 55° (Jans, 1979). The 02/12–lens is a maximum of $d = 1.28$ mm at its largest prism.

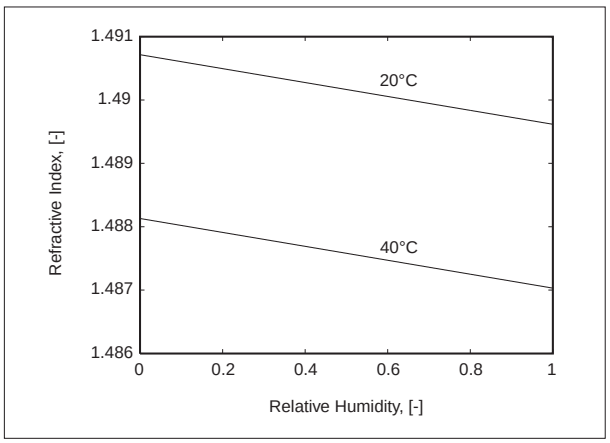

Figure 5: Dependency of refractive index of PMMA on relative humidity and temperature.

The refractive indices of plastics are temperature and humidity dependent. The effects of changes in relative humidity are smaller than the effects of changes in ambient temperature on the refractive index. Kouchiwa (1985) examined those changes for an injection molded polymethylmetacrylate singlet lens after having exposed it for a period of 30 days to changes from a defined standard condition of 20℃ and 65% relative humidity. He found an empirical equation including both the effects of temperature and relative humidity (Eqn. 4).

$$n_D = n_0 - 1.25 \cdot 10^{-4} \Delta t - 2.1 \cdot 10^{-7} \Delta t^2 - 1.1 \cdot 10^{-3} \Delta rh \quad (4)$$

where Δt, and Δrh are the changes in temperature and relative humidity from the standard condition. Kouchiwa's original formula (Eqn. 4) has been plotted for two temperatures 20℃ and 40℃ over the range of relative humidity in Fig. 5.

The transition temperatures of PMMA are relatively low at 266 K for glass, 399 K for rubber, while the range for melting is at 433-473 K (Pethrick, 1991). The effects on refractive index induced by changes in temperature and relative humidity for Fresnel lenses in actual applications can be neglected, as the effects are small, unless very high accuracy in imaging devices is required. The lens may serve as outer cover of the collector, and is air cooled.

5 COLOR BEHAVIOUR OF THE 02/12–LENS

Before we describe the pattern of wavelength dependent refraction at the nonimaging Fresnel lens, we shall calculate how the receiver is illuminated when light is incident from different directions. All light entering the lens aperture within the acceptance half angle pairs is refracted towards the absorber. This is true for each of the prisms constituting the lens: one may imagine an upside–down pyramid of light on any given point on the prisms' surfaces contributing to the light hitting the absorber.

Not all light, even after the losses on and inside the lens body are accounted for, reaches the absorber. Some rays miss, because of a combination of design principle and refractive laws. The design angles for the lens are the maximum combinations of the acceptance half angles, $+\theta/\psi$, and $-\theta/\psi$. The perpendicular angle ψ is symmetrical along the 2D–lens, but some rays entering at $\psi_{in} < \psi$, and maximum θ, are missing the absorber because refraction does happen in the perpendicular plane as well as it does happen in the cross–sectional plane of the lens.

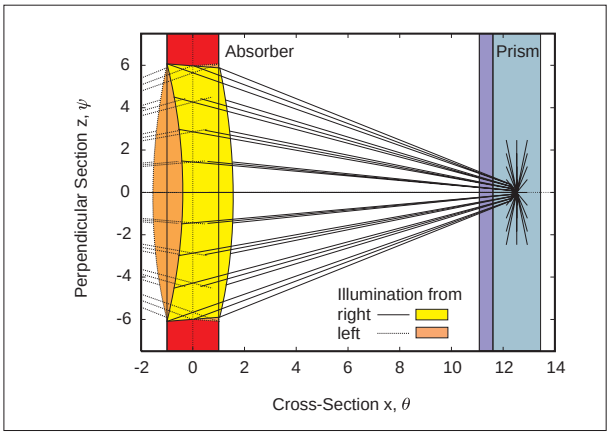

Figure 6: Top view of examplatory prism and absorber of the nonimaging Fresnel lens with acceptance half angle pairs $\pm\theta = 2°$ and $\pm\psi = 12°$. Incident light fills out an upside–down pyramid on any point of the lens, is refracted twice at the prism's faces, and shown intersecting the absorber level, where rays form a curved band of light due to perpendicular refraction. Oversized prism, for yellow light, refractive index $n = 1.49$.

Rays entering the lens, their refraction at the front and back faces of the prism and their intersection with the plane of the absorber have been pictured in Fig. 6. In this top view of an examplatory prism of the 0212–lens, it is clearly shown that the band of light incident on the absorber level is curved, and some rays incident at perpendicular angles smaller that the perpendicular design angle miss the receiver. Fig. 6 has been drawn using data for yellow light, with the refractive index of 1.49 used throughout the design of the lens.

The curvature of the concentration band becomes stronger with increasing design acceptance half angle pair ψ. This is the reason why ψ cannot be increased beyond values reasonably comparing to the cross–sectional acceptance half angle θ. A large ψ is desirable from the viewpoint of capturing solar rays during one–axis tracking, where ψ should theoretically be $\pm 23.45°$. In the light of the previous discussion of the lens' concentration ratio $C = 1/\sin\theta$, the character of ψ as restricting the ability to concentrate in

this 2D–collector becomes evident (see Leutz *al.*, 1999). So does the need for ray tracing when determining the actual concentration ratio.

The incompleteness of illumination of the absorber can be fixed by employing a secondary concentrator, e.g. a Compound Parabolic Concentrator. The acceptance half angle of this concentrator depends on the position of the outermost prism of the lens $P(x, y)$, and the extent of the absorber d, enlarged by the maximum extent of the curved band in cross–sectional x–direction, or even for bands formed by light of extreme wavelengths, if desired. The absorber of the truncated lens becomes the first aperture of the secondary concentrator, whose acceptance half angle must exceed

$$\theta_{CPC,\,min} = \tan^{-1}\left(\frac{x + d_{max}}{y}\right) \qquad (5)$$

For the truncated prototype of the 0212–lens, this procedure results in a CPC of a minimum acceptance half angle pair of around 55°, which in turn yields a geometrical concentration ratio of 1.2. This illustrates that additional concentration after the optimum lens is hardly possible, although the incomplete illumination of the absorber can be corrected. The nonimaging Fresnel lens is approaching the ideal concentrator for $\psi \to 0$, neglecting losses.

Table 2: Polymethylmetacrylate: Refractive indices (Oshida 1961), transmittance (Fresnel Technologies, 1995). Solar spectral terrestrial irradiance (Amakawa and Kuwano, 1994), and cumulative solar spectral energy (Wiebelt and Henderson, 1979) for three wavelengths in the near ultraviolet (*uv*), yellow (*D*), and near infrared (*ir*) light.

	uv	D	ir
Wavelength, 10^{-6} m	0.35	0.6	1.5
Refractive index, –	1.515	1.49	1.48
Transmittance, %	0.80	0.94	0.30
Solar irradiance, W/m^2	483.6	1395.0	182.0
Cumulative energy, %	< 2	25	87

Adding color to these considerations allows for more accurate desciptions of the refraction at the prism. Following the data used in Fig. 4, values for refractive index, solar irradiance, transmittance and cumulative energy corresponding to ultraviolet, yellow, and infrared radiation are found, and listed in Tab. 2. Often, values describing the solar spectrum are found as bordering the visible (400-700 nm), or describing the working range of a particular photovoltaic semiconductor. The response range of crystalline silicone c–Si is 300-1200 nm, that of amorphous silicone a–Si 300-900 nm, while crystalline InGaP cells respond to 300-650 nm, GaAs cells to 300-880 nm, and Ge cells (with less conversion efficiency) to 300-1880 nm, respectively. Photovoltaic cells may be stacked to increase their spectral response range. For a detailed discussion see Rumyantsev (1997), or King *et al.* (1997).

The infrared part of the solar spectrum is of no great concern as PMMA remains transmittant, and the refractive index is almost constant for large wavelengths (not so in the far infrared). The ultraviolet part of solar irradiance is, while not being absorbed in PMMA with uv–enhanced transmittance (dotted line in Fig. 4 (middle)), refracted increasingly stronger than visible wavelengths.

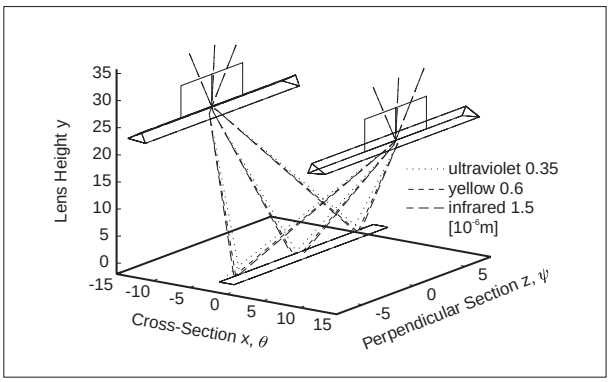

Figure 7: 0212–lens. Combinations of rays incident at $\theta = -2°$ and $\psi = -12, 0, +12°$ are drawn with refractions at symmetrical prisms, and intersections with the absorber level. Ultraviolet, yellow, and infrared rays roughly describing the extent of the solar spectrum, with corresponding refractive indices of polymethylmetacrylate.

In the three–dimensional Fig. 7 rays incident at combinations of $\theta = -2°$ and $\psi = -12, 0, +12°$ are drawn with refractions as well as intersections with the absorber level. Edge rays (those incident at design angles, and calculated with design refractive index) are hitting the edge of the absorber, while ultraviolet, or infrared rays are generally in greater danger to miss the absorber, although for the case of $\theta = -2°$ and $\psi = 0°$ from the left prism, the strong refraction of the ultraviolet ray let it reach the receiver while the design ray (yellow) misses.

The wavelength–dependent refractive power of a prism reaches a minimum for minimum deviation prisms. The angle of deviation is defined as the angle between the ray incident on the prism and the ray exiting the prism after two refractions. Although a prism can have only one angle of minimum deviation, the idea of 'reversible' prisms (Leutz *et al.*, 1999) used in the novel nonimaging Fresnel lens creates conditions for reduced dispersion.

Lorenzo (1981) evaluated chromatic aberrations in solar energy systems using Fresnel lenses. He found that lenses with acceptance half angles $\theta < 5°$ may lead to the refracted ray being spread wider than the width of the absorber. Considerations included the essentially nonimaging lens of Lorenzo and Luque (1981), and mention the possibility to correct chromatic aberrations. This can be done by arranging each prism individually, like in aspherical lens design. The absorber of an imaging design may be placed at what is called the 'cirle of least confusion' (CLC). Boise Pearson and Watson (1998) calculate the absorber position for this case explicitly, and credit Hecht (1990) with the definition of the CLC. The CLC is located where the refracted rays of the longest design wavelength from the right side of the lens, and the refracted ray of the shortest design wavelength from the left side of the lens (or vice versa) are intersecting (where 'right' and 'left' are the sides right and left of the optical axis of the system defined in a cross–sectional view). Using the CLC makes sense for actual imaging design where the focal area exceeds the ideal point, and an equivalent is useful in nonimaging design (see Eqn. 5).

However, rays missing the absorber are only a minor problem for photovoltaics, whereas inhomogeneous illumination due to shading or color separation is known to influence the electrical current and output of the photovoltaic cell.

Emphasis must be put on this second effect of color aberration, and the behaviour of the 2D–lens, where rays are incident within a pair of cross–sectional acceptance half angles $\pm\theta$ from both sides of the symmetrical lens, strongly influenced by the perpendicular acceptance half angle ψ, as was seen in Figs. 6, and 7. Presenting the rays in the latter in a cross–sectional projection, Fig. 8 is obtained. The yellow rays from both sides hit the edge of the receiver only when $\psi_{in} = \psi_{design}$. If the perpendicular incidence is not equal to the design angle, colors are mixing.

Since the usual case of operation of the nonimaging Fresnel lens is collecting solar rays incident anywhere within the acceptance half angle pairs, mixing of refracted, and color separated rays can be assumed. In fact, the concentrated sunlight on the absorber appears white in an experiment. It lacks the colors lining the focus characteristic to imaging Fresnel lenses that may be observed in a similar experiment conducted with conventional lenses, where the color aberrations increase with the rate of incidence deviating from the paraxial centerline of the optical system.

6 CONCLUSIONS

A novel nonimaging Fresnel lens has been presented in some detail, including preliminary tests of the lens under the full moon, which yield accurate visual results concerning the verification of the acceptance half angle design. The lens is manufactured as flat sheet lens, which is bent into shape. Both the design and manufacturing characteristics were found to be fulfilled highly satisfactory.

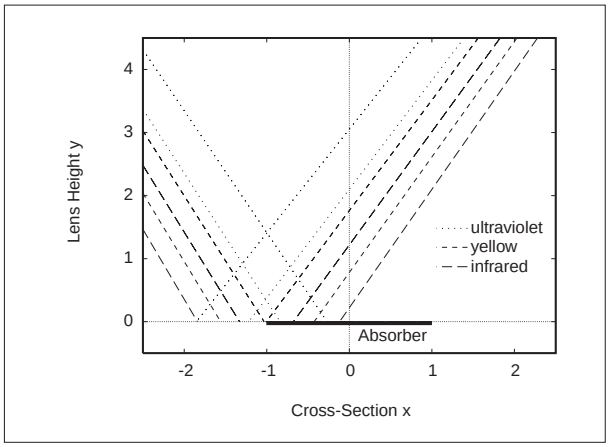

Figure 8: 0212–lens. Combinations of extreme rays incident at $\theta = -2°$ and $\psi = -12, 0, +12°$ are drawn with refractions at symmetrical prisms, and intersections with the absorber level. Ultraviolet, yellow, and infrared rays are mixing for incidence other than that at design angles. Cross–sectional projection.

The lens material, polymethylmetacrylate, is characterized according to temperature and humidity induced changes in its refractive index, which are found to be insignificant. Changes of the refractive index for wavelengths of the solar spectrum are more relevant for practical lens design, and are examined in detail.

Color aberration is not a major problem with the nonimaging 2D Fresnel lens concentrator. Not color induced inhomogeneous illumination, but incomplete illumination of the absorber must be regarded as being of prime importance, since colors separated by refraction at the prisms are usually mixed at absorber level, when the perpendicular incidence on the 2D–lens is taken into acount.

It is not necessary to develop a color corrected design approach for this type of nonimaging Fresnel lens. The incomplete illumination of the absorber may call for the use of a secondary concentrator, which only marginally increases the geometrical concentration ratio of the system, but ensures complete illumination of the absorber. The nonimaging lens is thought to be a suitable concentrator for photovoltaic and solar thermal applications.

7 REFERENCES

K. Amakawa, Y. Kuwano (1994) Solar Energy Engineering—Photovoltaics; Advanced Electronics Series I-3, Tokyo

E. C. Boes, A. Luque (1992) Photovoltaic Concentrator Technology; in: T. B. Johansson, H. Kelly,

A. K. N. Reddy, R. H. Williams (eds.): Renewable Energy, Sources for Fuel and Electricity, Washington, D. C.

J. Boise Pearson, M. D. Watson (1998) Analytical Study of the Relationship Between Absorber Cavity and Solar Fresnel Concentrator; *Proceedings of the International Solar Energy Conference; ASME*, 351-356, 14-17 June, Albuquerque, NM

M. Collares–Pereira (1979) High Temperature Solar Collector with Optimal Concentration: Non–Focusing Fresnel Lens With Secondary Concentrator; *Solar Energy* **23**, 409-420

Fresnel Technologies, Inc. (1995) Fresnel Lenses; brochure available at *http://www.fresneltech.com/html/products.html*, or Fresnel Technologies, Inc., 101 West Morningside Drive, Fort Worth, Texas 76110, USA

M. A. Green (1992) Crystalline– and Polycrystalline–Silicon Solar Cells; in: T. B. Johansson, H. Kelly, A. K. N. Reddy, R. H. Williams (eds.): Renewable Energy, Sources for Fuel and Electricity, Washington, D. C.

V. A. Grilikhes (1997) Transfer and Distribution of Radiant Energy in Concentration Systems; in: V. M. Andreev, V. A. Grilikhes, V. D. Rumyantsev: Photovoltaic Conversion of Concentrated Sunlight, Chichester

W. Grasse, H. P. Hertlein, C.–J. Winter (1991) Thermal Solar Power Plants Experience; in: C.–J. Winter, R. L. Sizmann, L. L. Vant–Hull (eds.) Solar Power Plants, Berlin

S. Harmon (1977) Solar–Optical Analyses of Mass–Produced Plastic Circular Fresnel Lens; Technical note, *Solar Energy* **19**, 105-108

E. Hecht (1990) Optics, Reading, MA

R. H. Hildebrand (1983) Focal Plane Optics in Far–Infrared amd Submilimeter Astronomy; *Proceedings of the SPIE—The International Society for Optical Engineering, Volume 441, International Conference on Nonimaging Concentrators*, 40-50, 25-26 August, San Diego, CA

R. W. Jans (1979) Acryclic Polymers for Optical Applications; *Proceedings of the Society of Photo–Optical Instrumentation Engineers (SPIE), Volume 204, Physical properties of Optical Materials*, 1-8, 27-28 August, San Diego, CA

F. A. Jenkins, H. E. White (1981) Fundamentals of Optics, 4., international edn., Singapore

S. Kaneff (1996) Solar Thermal Power—A Historical, Technological, and Economic Overview; *Proceedings of the 34th Annual Conference, Australia and New Zealand Solar Energy Society*, 294-306, Darwin, NT

D. L. King, J. A. Kratochvil, W. E. Boyson (1997) Measuring Solar Sprectral and Angle–of–Incidence Effects on Photovoltaic Modules and Solar Irradiance Sensors; *Proceedings of the 26th IEEE Photovoltaic Specialists Conference*, 29 September–3 October, Anaheim, CA, also at *http://www.sandia.gov/pv/ieee.html*

T. Kouchiwa (1985) Design of a Plastic Lens for Copiers; *Proceedings of the SPIE 1985 International Lens Design Conference*; *Volume 554*, 419-424, 10-13 June, Cherry Hill, NJ

E. M. Kritchman, A. A. Friesem, G. Yekutieli (1979) Efficient Fresnel Lens for Solar Concentration; *Solar Energy* **22**, 119-123

R. Leutz, A. Suzuki, A. Akisawa, T. Kashiwagi (1999) Design of a Nonimaging Fresnel Lens for Solar Concentrators; *Solar Energy* **65**, 6, 379-388

G. Löf (ed.) (1992) Active Solar Systems, *Preface*, Cambridge, MA

E. Lorenzo (1981) Chromatic Aberration Effect on Solar Energy Systems Using Fresnel Lenses; *Applied Optics* **20**, 21, 3729-3732

E. Lorenzo, A. Luque (1981) Fresnel Lens Analysis for Solar Energy Applications; *Applied Optics* **20**, 17, 2941-2945

O. E. Miller, J. H. McLeod, W. T. Sherwood (1951) Thin Sheet Plastic Fresnel Lenses of High Aperture; *Journal of the Optical Society of America* **41**, 11, 807-815

M. J. O'Neill (1978) Solar Concentrator and Energy Collection System; United States Patent 4069812

I. Oshida (1961) Step Lenses and Step Prisms for Utilization of Solar Energy; *New Sources of Energy, Proceedings of the Conference, United Nations*, Vol. 4, S/22, 598-603, 21-31 August, Rome

R. A. Pethrick (ed.) (1991) Polymer Yearbook 8, Chur

V. D. Rumyantsev (1997) Luminescent Phenomena in Concentrator Solar Cells; in: V. M. Andreev, V. A. Grilikhes, V. D. Rumyantsev: Photovoltaic Conversion of Concentrated Sunlight, Chichester

G. Sala, J. C. Arboiro, A. Luque, J. C. Zamorano, J. C. Miñano, C. Dramsch, T. Bruton, D. Cunningham (no year) The EUCLIDES Prototype: An Effficient Parabolic Trough for PV Concentration; http://www.users.globalnet.co.uk/~blootl/trackers/eucl.htm

Schott (1992) SCHOTT Computer Glaskatalog 1.0, Schott Glaswerke Mainz

R. R. Shannon (1997) The Art and Science of Optical Design, Cambridge

W. T. Welford, R. Winston (1989) High Collection Nonimaging Optics, San Diego

J. A. Wiebelt, J. B. Henderson (1979) Selected Ordinates for Total Solar Radiation Property Evaluation from Spectral Data; *Transactions of the ASME, Journal of Heat Transfer* **101**, 101-107